JOURNAL OF GEOPHYSICAL RESEARCH, VOL. 115, A04308, doi:10.1029/2009JA014929, 2010

Escape probability of Martian atmospheric ions: Controlling effects of the electromagnetic fields

Xiaohua Fang,[1] Michael W. Liemohn,[2] Andrew F. Nagy,[2] Janet G. Luhmann,[3] and Yingjuan Ma[4]

Received 24 September 2009; revised 1 November 2009; accepted 18 November 2009; published 15 April 2010.

[1] This study quantifies several factors controlling the probability of a pickup oxygen ion to escape from the Mars upper atmosphere. It is commonly presumed that ions with sufficient kinetic energy are able to escape to space. To test the validity of this simple assumption, we examined results from our Monte Carlo model, which monitors the motion of billions of test particles due to gravity and the Lorentz force through the electromagnetic fields of a magnetohydrodynamic model solution. It is shown that the electromagnetic fields are the dominant factor, surpassing the deceleration of gravity, in controlling ion transport and thus determine whether particles ultimately escape Mars or return to the planet. The particle kinetic energy and the local time of the crustal fields are also important factors greatly influencing the escape probability. In a simulation case in which the strongest crustal fields face the Sun at nominal solar minimum conditions, on average, only 45% of isotropically distributed newborn particles at ~400 km altitude are able to escape, even with a sufficiently high initial energy of ~10 eV. Furthermore, there is a distinct hemispheric asymmetry in the escape probability distribution, as defined by the upstream convection electric field direction ($\mathbf{E}_{sw}$). In the above case, the particles produced in the $-\mathbf{E}_{sw}$ hemisphere have a much smaller chance to escape, on average, about 17%. These findings imply that one has to be careful when using satellite periapsis measurements to estimate atmospheric loss, where ion densities are high but escape chances may be very low.

Citation: Fang, X., M. W. Liemohn, A. F. Nagy, J. G. Luhmann, and Y. Ma (2010), Escape probability of Martian atmospheric ions: Controlling effects of the electromagnetic fields, *J. Geophys. Res.*, *115*, A04308, doi:10.1029/2009JA014929.

1. Introduction

[2] One of the most challenging scientific problems of Mars is to understand how the planet dramatically changed from a dense, wet, and warm atmosphere about 3.5 billion years ago [e.g., *Carr and Wänke*, 1992] to the dry and cold present atmosphere. The loss of atmospheric particles to space, in particular, the loss of oxygen, has been identified as a major driver behind this change. In order to accurately backward extrapolate the climate evolution history, it is critical to have a clear picture of atmospheric loss for the present planetary and solar conditions, which can be theoretically modeled and tested by observations.

[3] Since the historic Viking missions more than three decades ago, tremendous observational efforts have been devoted to understanding the plasma and neutral atmospheric structures at Mars, and to estimating the atmospheric escape rates for present-day Mars [*Lundin et al.*, 1990; *Verigin et al.*, 1991]. The recent Mars Express mission provides an unprecedented opportunity to probe the charged particle distribution in the context of the Mars-solar wind interaction [*Lundin et al.*, 2004; *Barabash et al.*, 2007a]. For the estimates of planetary heavy ion loss at low altitudes, the focus of previous studies is on the kinetic energies of accelerated/heated particles [*Ergun et al.*, 2006; *Dubinin et al.*, 2009a, 2009b]. It was usually presumed that ions above the exobase with upward velocities exceeding the gravitational binding energy are able to escape, in analogy with Jeans escape. However, this simple presumption is not tested yet. It will be shown later in this study that the presumption is not valid, as the effects of the electromagnetic fields in the vicinity of Mars are ignored by considering only this escape energy criterion. Considering the strong influence of the electromagnetic forces on particle transport [e.g., *Luhmann*, 1990; *Fang et al.*, 2008, 2010], it is important to examine how gravity and the Lorentz force compete with each other in determining the destiny of hot ions. While it has

[1] Laboratory for Atmospheric and Space Physics, University of Colorado at Boulder, Boulder, Colorado, USA.
[2] Space Physics Research Laboratory, University of Michigan, Ann Arbor, Michigan, USA.
[3] Space Sciences Laboratory, University of California, Berkeley, California, USA.
[4] Institute of Geophysics and Planetary Physics, University of California, Los Angeles, California, USA.

0148-0227/10/2009JA014929

been pointed out by numerical models that an important part of energetic heavy ions cannot escape but crash back to the atmosphere of the planet [*Luhmann and Kozyra*, 1991; *Kallio and Koskinen*, 1999; *Fang et al.*, 2008], little is known, in quantitative terms, about the escape probability and its spatial location dependence.

[4] While Mars does not have a strong, intrinsic dipole magnetic field like Earth, it was revealed by the findings of the Mars Global Surveyor spacecraft that crustal magnetic anomalies exist for present-day Mars [*Acuña et al.*, 1998]. The nonuniform distribution of the crustal magnetic fields and their local time change due to the rotation of the planet complicate the Mars-solar wind interaction, and thus affect charged particle transport around Mars. In the very recent studies by *Fang et al.* [2010] and *Li and Zhang* [2009], the roles of the crustal fields in the escape ion flux distribution far down the tail have been discussed. It is illustrated by *Fang et al.* [2010] that the total ion escape rate in the tail region can be altered by more than a factor of 2 by simply changing the local time of the crustal fields. It is still not clear, however, the extent to which the ion escape probability in the source regions at low altitudes is affected by the crustal fields. In this work, we investigate how the escape probability of ions depends on the Martian electromagnetic environment by changing the local time of the crustal fields in numerical simulations.

[5] Owing to the lack of a strong intrinsic magnetic field and the weakness of the local interplanetary magnetic field (IMF) at 1.5 AU, the gyroradius of ions can be comparable to or even larger than the planetary scale. As a consequence, a hybrid model [e.g., *Brecht*, 1997; *Kallio and Janhunen*, 2002; *Modolo et al.*, 2005] or a test particle model [e.g., *Luhmann*, 1990; *Kallio and Koskinen*, 1999; *Cravens et al.*, 2002; *Fang et al.*, 2008] is expected to be more appropriate than a magnetohydrodynamic (MHD) model in resolving the heavy ion gyroradius effects during particle transport at Mars. However, current computational resources are not sufficient to solve the solar wind and ionosphere/atmosphere interaction processes completely self-consistently. The typical number of particles per cell in the existing hybrid models is low and therefore detailed chemistry calculations are not included particularly well at low altitudes. In this sense, a combined MHD and test particle model is a valuable alternative to hybrid models, as many more particles can be used in the simulation domains. In particular, a test particle approach has the capability of resolving the ion flux distribution throughout phase space, i.e., in both real space and velocity space, everywhere around Mars [*Fang et al.*, 2008].

[6] In this work, we apply the recently developed MHD field-based test particle model [*Fang et al.*, 2008, 2010] to quantitatively investigate the role of the electromagnetic fields (including the crustal fields) in the ion escape probability distribution at Mars. In section 2, brief descriptions are given of the models used in our numerical simulations. The findings are reported in section 3. A discussion and conclusion follows in section 4.

2. Model Description

[7] The main tool for this study is our recently developed Monte Carlo ion transport model that tracks the motion and acceleration of pickup ions through near-Mars space. The model has been described in detail by *Fang et al.* [2008]. Here we briefly outline its major components.

[8] In the model, the ion motion is determined by solving Newton's equation

$$m\frac{d^2\mathbf{r}}{dt^2} = e\frac{d\mathbf{r}}{dt}\times\mathbf{B} + e\mathbf{E} - \frac{GMm}{r^2}\mathbf{e}_\mathbf{r}, \tag{1}$$

where $\mathbf{r}$ is the location of a particle and e is the electric charge with the assumption that oxygen is singly ionized. The third term on the right-hand side of the equation represents the gravity force, and $\mathbf{B}$ is the background magnetic field, determined from a 3-D multispecies MHD model of *Ma et al.* [2004]. Also $\mathbf{E}$ is the convection electric field, derived from the MHD bulk plasma velocity ($\mathbf{U}$) and the magnetic field, that is,

$$\mathbf{E} = -\mathbf{U}\times\mathbf{B}. \tag{2}$$

It is worth noting that in our current model, the Hall electric field ($\mathbf{j}\times\mathbf{B}/(en_e)$) and the polarization electric field (mainly $-\nabla p_e/(en_e)$) are neglected, where n_e and p_e stand for the electron number density and thermal pressure, respectively. The Hall term of the electric field was suggested by *Lichtenegger et al.* [1995] to reproduce low-energy oxygen ion flux observations close to the central wake of Mars, while the polarization electric field was proposed by *Hartle and Grebowsky* [1995] for light ion upward flows in the Venusian nightside ionosphere and then invoked by *Barabash et al.* [2007b] to explain the observed feature of mass-independent energy spectra at Venus. It is interesting to follow test particle motion with all the three electric field terms taken into account and quantitatively evaluate their relative contributions in determining particle distributions. However, not enough work has been done on this aspect. It is not clear how the escape probability of pickup ions is altered when the Hall and polarization electric fields are included in the particle motion equation. This requires further investigation but is beyond the scope of the present study.

[9] Note that the test particle approach does not take into account the electromagnetic field perturbations along with the particles; that is, there is no feedback to the background electromagnetic environment in our simulations. This assumption is appropriate as long as the MHD model accurately describes the macroscopic properties of the Mars-solar wind interaction. It has been shown that MHD models are generally successful in reproducing many observed features, such as the locations of the bow shock and the ionopause [*Ma et al.*, 2004; *Harnett and Winglee*, 2006].

[10] In this study, the electromagnetic environment of near-Mars space is derived using the *Ma et al.* [2004] MHD model for nominal solar minimum conditions. In the MHD model, the lower boundary is taken to be 100 km above the Martian surface, well below the peak altitudes of major ionospheric constituents. The ion densities at the lower boundary are determined under a photochemical equilibrium assumption. Given the small altitude resolution of 10 km and the inclusion of comprehensive chemistry, the MHD model self-consistently includes and calculates the Martian ionosphere by considering both chemistry and transport

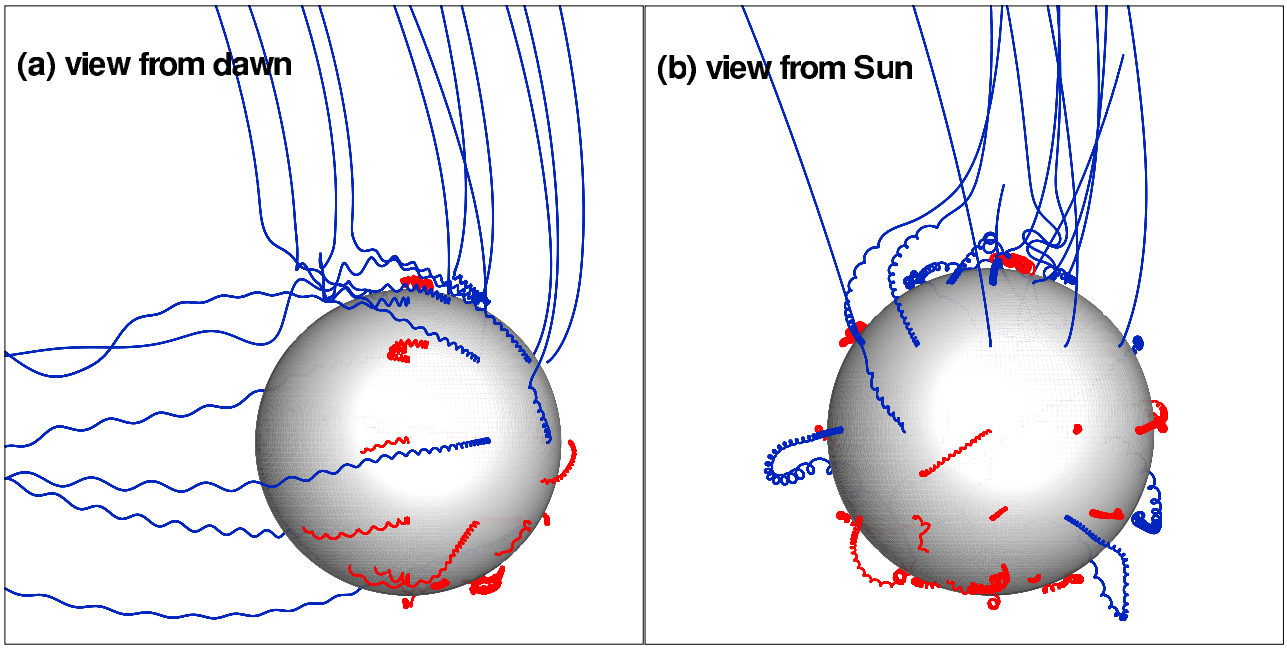

Figure 1. Orthogonal views of the trajectories of sample ions that are emitted radially outward at 400 km altitude on the dayside with an initial energy of 10 eV. The strongest Martian crustal fields face the Sun. The colors mark the particles that ultimately escape from the $r = 5\ R_M$ boundary (blue) or crash back into the atmosphere (red), respectively.

processes. It has been illustrated by *Ma et al.* [2004] that the MHD-calculated ionosphere is consistent with observations. Therefore, the MHD model provides realistic electromagnetic fields within its limitation by taking into account currents everywhere (including the ionosphere). In the model setup, the IMF in the upstream solar wind is a Parker spiral at 56° angle from the Sun-Mars line. The IMF magnitude is 3 nT. The solar wind density and speed are set to be 4 cm^{-3} and 400 km s^{-1}, respectively. The crustal magnetic fields of Mars are specified using the *Arkani-Hamed* [2001] model. To investigate how crustal anomalies affect the electromagnetic environment and thus the ion escape probability, their local time will be changed from the dayside (case 1) to the dawnside (case 2) and when the crustal sources are removed from the simulations (case 3) [*Ma et al.*, 2004; *Fang et al.*, 2010].

[11] There are three ion production processes incorporated in our test particle model: ionization of the Martian oxygen corona from solar EUV radiation, charge exchange collisions with ions, and impact ionization by solar wind electrons. The simulation domain for tracking newborn ions extends from the exobase altitude (200 km in accordance with solar minimum conditions by *Nagy et al.* [2001]) up to 5 Martian radii (1 R_M = 3396 km) away from the planet center. The ions are followed up to 3000 sec until they are lost, either by escaping from the outer spherical boundary or by falling back into the inner boundary. No collision loss is considered during particle transport, as the collision frequency is sufficiently low at altitudes above the exobase.

[12] In the model, test particles are launched into the simulation domain according to a specified number of particles per source cell. The source grids are uniformly spaced with respect to the natural logarithm of the radial distance. This results in a vertical spatial resolution of approximately 36 km at the bottom and 168 km at the top. The other two spherical coordinates are typically defined with a 5° resolution in longitude and latitude, making a total of 156 × 36 × 72 spherical cells in the domain. To obtain the ion escape probability with enough statistics, 5000 test particles are used per source cell in this study, resulting in about 2 billion particles in the whole domain. In order to accomplish the computational requirements, our test particle code is highly parallel using a sophisticated dynamic load balancing strategy.

[13] Unless otherwise specified, all newborn pickup ions are assumed to have an isotropic angular distribution. That is, the numbers of particles emitted outward and inward are approximately equal. Initially, newborn particles have a Maxwellian energy distribution, with the temperature equal to that of the local neutral atmosphere, i.e., 198 K in the simulated solar minimum conditions. However, the energy with the most probable speed in this distribution is very low, only about 0.02 eV. In numerical simulations, an artificial initial energy (≤10 eV) is commonly used [e.g., *Luhmann*, 1990; *Kallio and Koskinen*, 1999; *Kallio and Janhunen*, 2002; *Fang et al.*, 2008]. In this study, in addition to the low-energy part that is described by the Maxwellian distribution (which actually can be neglected), newly created particles obtain an extra constant kinetic energy. The value of this additional energy is an experimental parameter and is varied as 1 eV, 10 eV, and 100 eV in the present study. Considering that the gravitational binding energy at 200 km altitude is about 2.0 eV, the comparison of the results with different initial energies can help understand the relative importance of gravity versus electromagnetic fields in ion escape at Mars. Given the fact that the artificially added initial energy is much larger than the one determined from the neutral atmospheric temperature, the extra constant energy

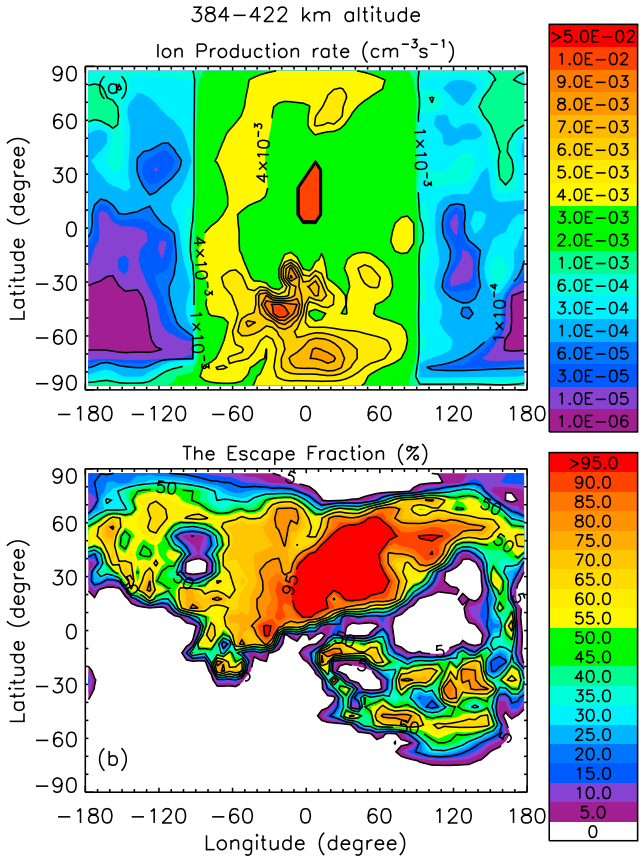

Figure 2. Horizontal distributions of (a) pickup oxygen ion production at 384–422 km altitudes, and (b) the corresponding escape fraction. The particles have an isotropic angular distribution with an initial energy of 10 eV. In this simulation case, the strongest crustal fields are on the dayside. The subsolar position is in the middle.

will be referred to as the initial energy for simplicity throughout the paper.

3. Results

[14] Figure 1 shows sample pickup O^+ trajectories in case 1, in which the subsolar location of Mars is at 180°W and 0°N. That is, the electromagnetic fields are obtained from the MHD model with the strongest Martian crustal fields on the dayside near noon. The spatial distributions of the MHD-calculated magnetic field and convection electric field have been reported in detail by *Fang et al.* [2010], and are not repeated here. In simulations, the starting points of sample test particles are at 400 km altitude, and are evenly distributed on a 30° × 30° longitude-latitude grid. Because the nightside contributes to less than 5% ion production in total (through charge exchange and electron impact processes), we are primarily interested in the escape chances of the ions at low altitudes on the dayside. For the purpose of examining the competition between gravity and the electromagnetic force, the sample particles are launched radially outward with an initial energy of 10 eV, much larger than the local gravitational potential energy of 1.9 eV.

[15] As seen in Figure 1, 20 out of 37 sample test particles ultimately fall back to the atmosphere. That is, less than one half of particles can escape Mars in this example. In other words, the dayside averaged ion escape probability at 400 km altitude may be less than 50% (note that the sample particle distribution is not exactly reflective of real ion production). It should be pointed out that this phenomenon cannot be explained by considering only gravity, as all the particles are supposed to have sufficient energy to overcome gravity. Rather, it sheds light on the effects of the electromagnetic fields in particle transport and thus their importance in atmospheric erosion.

[16] In addition, a remarkable asymmetry exists in the hemispheric distribution of escaping particles. Most of sample particles originating in the Northern Hemisphere are able to escape, except some starting at the terminator. In contrast, most of the particles in the Southern Hemisphere cannot obtain much acceleration and eventually crash back to the atmosphere. Note that the convection electric field upstream of Mars (hereinafter referred to as $\mathbf{E}_{sw}$) points toward the north for the simulated solar wind conditions. The hemispheric asymmetry in particle transport resulting from the electromagnetic fields has been reported in previous studies [e.g., *Luhmann*, 1990; *Brecht*, 1997; *Fedorov et al.*, 2006; *Fang et al.*, 2008]. Again, the asymmetric distribution highlights the importance of the electromagnetic environment near Mars, as the gravitational force is assumed to be spherically symmetric.

[17] In Figure 1, the ion escape probability distribution is clearly but roughly outlined. A quantitative investigation is undertaken, and the results are shown in Figure 2, in which the horizontal distributions of the ion production rate and the escape fraction are presented. The escape fraction is defined as the number of particles that are able to escape Mars divided by the total number of particles in a unit volume. In the numerical calculations, the number of escaping test particles following production is accumulated and then divided by total particles in a cell (i.e., 5000). By this means, the fraction is a statistical quantity that represents the probability of a newborn pickup ion that can escape to space. Similar to the definition of the escape fraction, the return fraction at a source location is defined to be the proportion of pickup ions in a unit volume that ultimately fall back to the atmosphere. By taking a maximum particle tracing time of 3000 s in our model, the proportion of the particles that obtain no significant acceleration and stay in the interior of the computational domain during their lifetime is reasonably negligible [*Fang et al.*, 2008]. Therefore, the return fraction at a source location is simply 100% minus the escape fraction. In this study, we will also examine the escape and return fractions averaged over the half-spherical shells on the dayside, or over the quarter-spherical shells in the dayside Northern and Southern hemispheres. The average escape (return) fraction is defined to be the ratio of the total escaping (returning) particles to the total pickup ions in the shell volumes.

[18] Here we follow the pickup ions created within a certain spherical shell in the simulations, which is between 384 km and 422 km altitude. The particles initially are assumed to have an isotropic angular distribution with an energy of 10 eV. It is seen in Figure 2a that the dayside atmosphere provides the majority of pickup ion source. Because of the existence of the dayside strong crustal fields and their influences on the plasma flow, the ion production

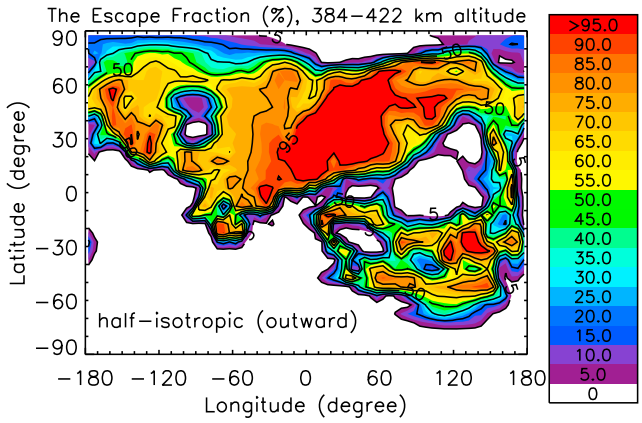

Figure 3. Horizontal distribution of the ion escape fraction. Similar to Figure 2b, but assuming a half-isotropic angular distribution; that is, all particles initially move outward.

rate slightly deviates from a symmetric distribution about the Sun-Mars line. Figure 2b shows that for 10 eV and isotropically distributed particles, the average ion escape probability at around 400 km altitude is 44.9% on the dayside, close to the rough estimate obtained from Figure 1. Also, as expected from the interpretation of Figure 1, there are distinct differences in the ion escape probability between the Northern and Southern hemispheres, which are quantitatively illustrated in Figure 2b. The simulation results show that, on average, pickup ions created at ~400 km altitude in the Northern (i.e., $+\mathbf{E}_{sw}$) Hemisphere on the dayside have a 73.5% probability to be lost to space. In contrast, the average number dramatically drops to 17.3% in the Southern (i.e., $-\mathbf{E}_{sw}$) Hemisphere. If we consider individual source locations, the hemispheric asymmetry is more apparent. There are broad regions in the Southern Hemisphere with a <5% escape probability, while there are also broad regions in the opposite hemisphere with an escape probability of >95%. This striking difference occurs despite particles having the same initial energy, one that is sufficient to overcome gravity. The results that the particles in the $+\mathbf{E}_{sw}$ hemisphere are much easier to escape indicate the controlling effects of the electromagnetic fields. It is illustrated that the motion of particles is mainly governed by the Lorentz force, instead of gravity, in the near-Mars space. Therefore, an atmospheric loss estimate considering only particle kinetic energies is far from enough.

[19] To further demonstrate the negligible effects of gravity in ion transport, we consider a numerical experiment and assume that all the initial particles are now half-isotropically distributed. That is, no particles move inward. The recalculated escape fraction distribution at around 400 km altitude is presented in Figure 3, for comparison with Figure 2b. Because the results are so similar, it is inferred that gravity is not a controlling force in particle transport at Mars, because otherwise all of the ions should have escaped in this experiment. Rather than having a 100% escape fraction, the particles have a nearly identical escape probability distribution as in Figure 2, although with a slight enhancement for most of the values. The escape probability averaged over the whole dayside shell increases a little to 47.2%, with the average values in the Northern (Southern) Hemisphere becoming 76.2% (19.0%). The similarity between Figures 2 and 3 indicates that it is indeed the electromagnetic fields that surpass the deceleration of gravity and determine whether a pickup ion is able to escape Mars.

[20] The previous simulation results are for particles initially starting at, or close to, 400 km altitude. In Figure 4, the ion escape fraction is shown as a function of source altitude in the equatorial plane and in the noon-midnight meridional plane, complementing the results in Figure 2. It is seen that the pronounced hemispheric asymmetry exists at all altitudes, not only at around 400 km. There is also a dawn-dusk asymmetry evident in the ion escape probability distribution, as the crustal fields are not symmetric about the noon-midnight meridional plane.

[21] Figure 5 provides a global picture of pickup ion production and escape/return fractions within the Martian electromagnetic environment. Here, the focus is placed on the values averaged over the spherical shells on the dayside and on their dependence on the source altitude. It is seen in Figure 5b that the dayside averaged escape fraction (blue curve) quickly increases from 10.5% at 200 km altitude to 78.4% at around the magnetic pileup boundary (MPB, approximately 750 km altitude at the subsolar point in this case). Above the MPB, there are no significant variations in the escape/return fraction. This is consistent with the findings of *Fang et al.* [2008], who found that the strong convection electric field outside of the MPB (particularly in the

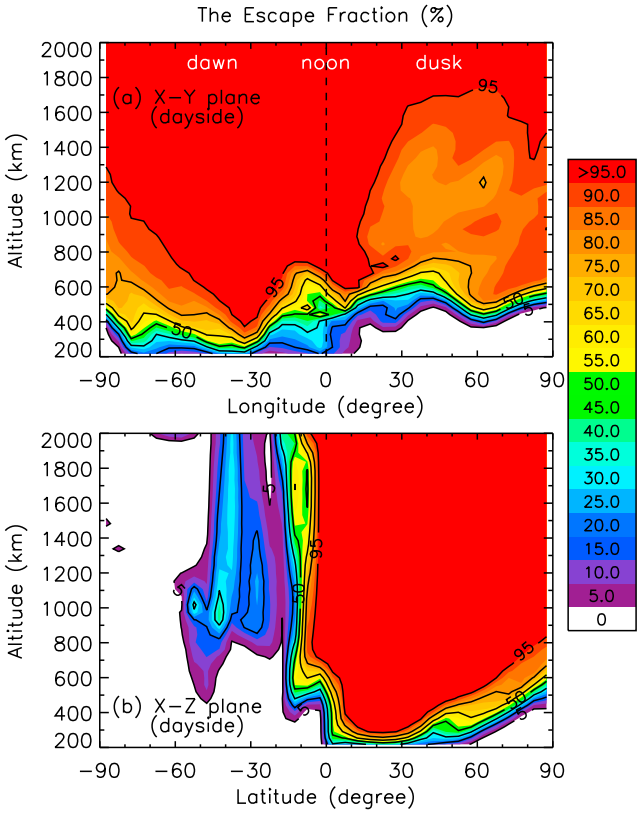

Figure 4. Vertical distributions of the ion escape fraction in (a) the equatorial plane and (b) the noon-midnight meridional plane. Initial particles are assumed to have an isotropic angular distribution with an energy of 10 eV. The local time of the strongest crustal field is at noon.

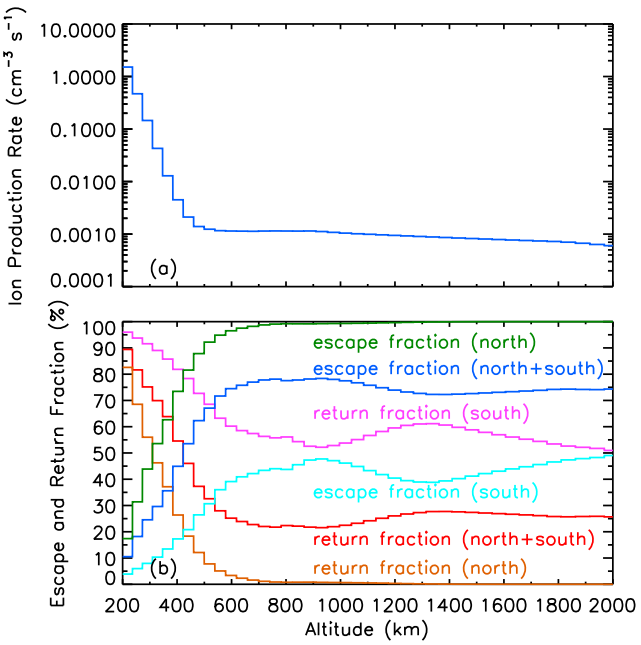

Figure 5. (a) Dayside-averaged pickup oxygen ion production rates, and (b) ion escape and return fractions averaged over the dayside and over the dayside Northern (i.e., $+\mathbf{E}_{sw}$) and Southern (i.e., $-\mathbf{E}_{sw}$) hemispheres, as a function of source altitude. In the calculations, $E_0 = 10$ eV. The strongest crustal magnetic fields are on the dayside.

magnetosheath region) is favorable to the pickup ion acceleration. It shows that in order to estimate atmospheric loss, the electromagnetic fields are crucial and have to be considered. Also, in Figure 5b, the hemispheric asymmetry in the ion escape and return fractions are summarized by comparing the average values in the quarter-spherical shells in the $+\mathbf{E}_{sw}$ and $-\mathbf{E}_{sw}$ hemispheres. It is seen that the difference in the average escape/return fraction between the two hemispheres gradually increases with altitude, reaches its maximum approximately at MPB, and then remains at that level for higher altitudes.

[22] In previous simulations, we consider the electromagnetic environment with the strong crustal magnetic anomalies on the dayside and test particles with an initial energy of 10 eV. It is also interesting to investigate how the distribution of the pickup ion escape probability responds to the change in the particle initial energy. Numerical experiments were conducted here by assuming different initial energies, ranging from 1 to 100 eV, for all the ions within the simulation domain. These artificially imposed energies may be partially reflective of different initial ion heating intensities as described by *Ergun et al.* [2006]. The results of such calculations are presented in Figure 6a. It is shown that the responses of the ion escape probability to initial energy changes are most pronounced at low altitudes. In particular, the escape fraction at around 200 km altitude increases from 6.5% to 10.5% and to 13.7% when E_0 increases from 1 eV to 10 eV and to 100 eV, respectively. If gravity were the dominant factor in determining particle transport, then the particles with E_0 of 10 or 100 eV should have an identical escape probability. Note that there is basically no change in a broad region below 1000 km altitude between the $E_0 = 10$ eV and $E_0 = 100$ eV simulation results. Actually, ions have a little smaller chance to escape, on average, at altitudes of ~300–400 km, when E_0 increases from 10 to 100 eV. This is the consequence of two different effects. As the initial energy increases, particles have a larger gyroradius in the electromagnetic fields. Therefore, particles are governed by the Lorentz force in a larger region. This effect is complicated, because the electromagnetic fields are spatially dependent. In addition, the downward moving particles with a larger velocity may be more liable to be lost by impacting the low-altitude atmosphere.

[23] The Martian crustal magnetic fields not only regionally deflect the incoming solar wind plasma [*Mitchell et al.*, 2001] but also have an important global effect on the Mars-solar wind interaction [*Brain et al.*, 2005] and on the spatial distribution of escaping pickup ion fluxes in the tail region [*Fang et al.*, 2010]. As the local time of the crustal fields (and thus the standoff pressure of the planetary obstacle) changes, the position of the Mars-solar wind interaction region correspondingly changes [*Crider et al.*, 2002; *Verigin et al.*, 2004]. This process can result in a significant change in the total ion escape rate in the tail region by more than a factor of 2 [*Fang et al.*, 2010]. In this study, the crustal field effects are studied for their impact on the ion escape probability with respect to source altitude by changing their local times, and are illustrated in Figure 6b.

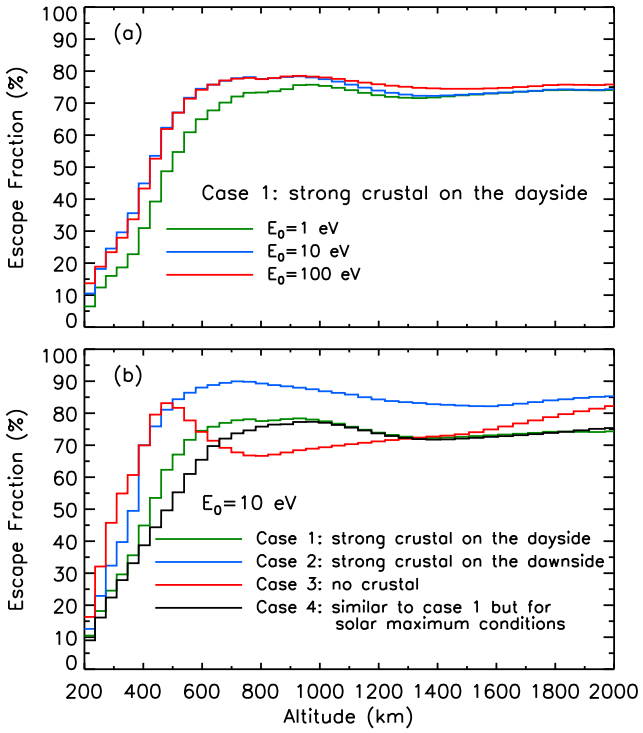

Figure 6. Dayside-averaged escape fractions of pickup oxygen ions with respect to source altitude. (a) Electromagnetic fields are from the MHD model with the strongest crustal fields on the dayside, while the initial energy of particles is varied: 1 eV, 10 eV, and 100 eV. (b) Initial energy is set to be 10 eV while the local time of the crustal fields is changed. The black curve shows the results in a case similar to case 1 but for nominal solar maximum conditions (see text).

Table 1. Average Escape Probability (%) of Oxygen Ions at 384–422 km Altitudes on the Dayside for Different Initial Energies and in Different Simulation Cases[a]

	E_0 = 1 eV			E_0 = 10 eV			E_0 = 100 eV		
	case 1[a]	case 2	case 3	case 1	case 2	case 3	case 1	case 2	case 3
Dayside, total	30.9	67.2	69.0	44.9	70.0	70.0	43.3	65.8	59.3
Dayside, $+\mathbf{E}_{sw}$ hemisphere	60.3	89.0	85.8	73.5	92.1	90.5	67.2	89.2	79.1
Dayside, $-\mathbf{E}_{sw}$ hemisphere	2.5	30.8	52.0	17.3	33.1	49.2	20.2	26.8	39.1

[a]case 1, strong crustal fields on the dayside; case 2, strong crustal fields on the dawnside; case 3, no crustal fields.

As already seen from Figure 5, the escape fractions tend to quickly increase to their peak values and then remain at a high level. When the local time of the crustal fields changes from the dayside (case 1) to the dawnside (case 2) and even more so when the crustal sources are removed from the simulations (case 3), the pressure (and thus the effective obstacle size) is weakened with an inward-moving MPB [*Ma et al.*, 2004; *Fang et al.*, 2010]. This is reflected in Figure 6b, which shows that the peak escape fraction altitude correspondingly decreases. It is worth noting that during the local time changes from case 1 to case 2 and to case 3, pickup ions at low altitudes escape Mars more easily in general on the dayside. This is consistent with the fact that during these changes the solar wind can penetrate deeper, resulting in a stronger electromagnetic environment close to Mars. Also, the higher variation in the ion escape probability in Figure 6b than in Figure 6a indicates that the electromagnetic fields, rather than gravity, is a controlling factor in particle transport and escape.

[24] Although the present work is focused on nominal solar minimum conditions, it is useful to evaluate how changes in solar activity affect the capability of pickup ions to escape to space. For the purpose of a direct quantitative comparison, we add a new case (case 4) in which the Martian crustal field and solar wind conditions are exactly the same as in case 1, except that solar radiation and the planetary atmosphere are set to be appropriate for nominal solar maximum conditions [see *Ma et al.*, 2004; *Fang et al.*, 2008]. The simulation results of this new case for E_0 = 10 eV are presented in Figure 6b for a side-by-side comparison with the other solar minimum cases. It is clearly shown that the escape probability generally decreases from case 1 to case 4, notably at altitudes inside the MPB. This variation is understandable when we examine the change in the Mars-solar wind interaction in a similar way as described above for the changes among the three solar minimum cases. In case 4, photoionization rates as well as atmospheric densities are enhanced in accordance with the solar maximum conditions, resulting in a larger obstacle size and making mass loading of the solar wind start taking place at a further distance. The MPB subsolar point is located at about 815 km altitude, approximately 65 km higher than that in case 1. That is, the solar wind in case 4 cannot penetrate as deep as in case 1, resulting in relatively weaker electromagnetic fields in the vicinity of Mars. Therefore, it is not surprising to see that the dayside averaged escape fraction at ~400 km altitude drops from 44.9% in case 1 to 38.7% in case 4. Moreover, the peak altitude of the escape fraction is higher in the solar maximum case, reflective of the outward displacement of the MPB. Note that in these comparisons, the computational domain remains the same. If the inner spherical boundary moves from 200 to 300 km altitude for case 4 in accordance with the fact that the exobase is elevated from solar minimum to solar maximum [*Nagy et al.*, 2001], the escape probability at low altitudes will further decrease. This is because particles will be more liable to be lost by bombarding the low-altitude atmosphere and thus cannot escape to space. For example, the dayside averaged escape probability at ~400 km altitude will drop to 29.9% in case 4 if the inner boundary is elevated.

[25] It was speculated by *Ergun et al.* [2006] that ionospheric particles are thermally diffused to around 400 km altitude, obtain plasma wave heating, and are lost to space. As illustrated throughout this paper, whether particles can ultimately manage to escape is determined not only by gravity but most importantly by the electromagnetic fields in the vicinity of Mars. Here in Table 1, we quantitatively list the dayside-averaged ion escape fractions for energetic particles starting at plasma wave heating altitudes for a variety of conditions. The results are given for varying initial particle energies and for the simulation cases with different crustal field local times. Note that the escape probability of E_0 = 1 eV pickup oxygen ions is considerably greater than the gravitational escape probability (i.e., zero). If gravity were a controlling factor, we would expect to see no escape at all, as 1 eV is lower than the gravitational binding energy at 400 km altitude. In addition to providing the values that are averaged over the dayside, the escape fractions in different hemispheres are listed in Table 1 to illustrate the distinct hemispheric asymmetry. Particles in the $-\mathbf{E}_{sw}$ hemisphere are easily directed by the convection electric field back to the atmosphere and are lost. As seen in Table 1, on average, particles in the $-\mathbf{E}_{sw}$ hemisphere have a probability of as low as ≤20% to escape, even though particles are assumed to be initially heated to a significantly high level of 100 eV. It is worth pointing out that the results in case 2 and in case 3 are closer to each other than those in case 1. This is because case 2 and case 3 have similar dayside conditions of the crustal fields, and thus their electromagnetic environments in the dayside Mars-solar wind interaction region are closer to each other than either is to the conditions of case 1 (when the strongest crustal fields are on the dayside).

4. Discussion and Conclusion

[26] We have applied a recently developed MHD field-based test particle model to investigate the escape probability of pickup oxygen ions with respect to the source location. Throughout this study, we focus on the dayside ion production and transport. Our numerical simulations show that gravity is not a determining factor of whether particles are able to escape Mars or ultimately fall back to the low-altitude atmosphere. The problem with relying solely on particle

kinetic energies is that the dominant controlling factor, the electromagnetic environment in the near-Mars space, is not taken into account. The consequences of that omission can be very severe. This is particularly notable when one estimates ion escape using measurements at periapsis of satellites, where ion densities are high but escape probabilities are low.

[27] Let us take a specific example to assess how much the atmospheric loss estimate is affected by including the electromagnetic field effects. Following *Dubinin et al.* [2009a, 2009b], we assume a simple altitude profile of ion densities in a region where erosion takes place: $n = n_0\exp(-(h - h_0)/H)$, where $h_0 = 300$ km, and $H = 120$ km. Although the present study is undertaken for newborn ions, the derived escape probabilities actually do not have such a limitation. For particles at a given location, the key factors determining whether or not they are able to escape are their velocity (i.e., energy and moving direction) and the background electromagnetic environment. It does not matter whether particles are newly created or whether they move from other regions. Therefore, assuming that the ions in the atmospheric erosion region have an isotropic angular distribution with an energy of 10 eV, we can apply the altitude-dependent, dayside-averaged escape fraction distribution in Figure 5b to estimate their escape probability. The calculation results show that the column-averaged escape probability for the ions between 350 and 850 km altitudes is 53.4%. That is, nearly one half of ions actually crash back to the atmosphere and are not lost to space. Considering the hemispheric asymmetry, there is a much smaller column-averaged escape probability in the $-\mathbf{E}_{sw}$ hemisphere. In this case, the value is as low as 23.3%. Therefore, in order to appropriately estimate atmospheric loss, it is important to have a view of the global picture of the Mars-solar wind interaction in addition to the kinetic energy of atmospheric ions. The neglect of the electromagnetic field effects in particle transport leads to an overestimation of the ion escape rate. Although the overall error due to this neglect is roughly about a factor of 2 on the dayside, the escape rate in the $-\mathbf{E}_{sw}$ hemisphere may be overestimated by up to an order of magnitude. In this example, if atmospheric erosion under consideration takes place mainly in the $-\mathbf{E}_{sw}$ hemisphere, a correction factor of 0.233 has to be applied to the total ions in order to properly assess atmospheric loss.

[28] As illustrated by numerical models [e.g., *Luhmann*, 1990; *Fang et al.*, 2008, 2010], particle transport is primarily determined by the electromagnetic field distribution in the vicinity of Mars. As a consequence, the probability of ion escape highly relies on the electromagnetic environment, which, however, is dependent on a number of factors, such as the intensity of solar radiation, the solar wind conditions, the local time of crustal magnetic anomalies, and solar wind mass loading from the planetary atmosphere. Even with specified electromagnetic fields, the ion escape probability is not straightforward to evaluate. The probability is highly spatially dependent and has a distinct hemispheric asymmetry. Therefore, this complication requires a careful analysis under specific circumstances of interest in order to make reasonable atmospheric loss estimates using satellite measurements. A test particle model together with MHD or hybrid-model-calculated electromagnetic fields is suitable for such calculations. In our current model, the polarization electric field is neglected, which, however, was proposed by *Hartle and Grebowsky* [1995] to account for light ion upflows in the Venusian nightside ionosphere. Such a field was invoked by *Barabash et al.* [2007b] to explain observed ionospheric ion acceleration at low altitudes at Venus, where the convection electric field is weak. By adding this term to the electric field in the particle motion equation, it is expected that more ions will be propelled upward, leading to an enhancement in the ion escape probability. However, it is difficult, without resorting to detailed simulations, to determine the relative importance of the polarization electric field in particle transport. It is planned to include the polarization and Hall electric fields besides the convection term in our future model development. It will be useful to run our model with different electric field terms turned on or off, and make side-by-side comparisons of escaping ion flux distributions. The results of these investigations will enhance our understanding of particle transport in the complicated electromagnetic environment and thus help make more accurate predictions on atmospheric loss at Mars.

[29] Considering that the ion escape probability changes both vertically and horizontally, escaping particles measured far away from the planet are expected to consist of superimposed contributions from different low-altitude sources. It is proposed by *Fang et al.* [2008] that the pickup ion distribution in velocity space can be used to assess the possibility of determining the source location and mechanism of the pickup ions from high-altitude observations. This type of analysis requires a code such as the one we are using [*Fang et al.*, 2008, 2010], which launches a tremendous large number of test particles in the simulation to achieve a high-resolution distribution in both real space and velocity space. With the help of such numerical tools, measured escaping particles can be traced back within modeled electromagnetic fields to their original source regions. This is invaluable in providing physical insight into the details of atmospheric loss as seen in high-altitude ion observations.

[30] It should be pointed out that sputtering loss due to the bombardment of energetic pickup ions at low altitudes [*Luhmann and Kozyra*, 1991; *Johnson*, 1994; *Leblanc and Johnson*, 2001] is not taken into account. As a result, the ion escape probability values in this study are lower limits as additional escape caused by the momentum transfer of returning pickup ions is ignored. Also, the analyses in this study assume that no collisions occur during particle transport. The computational domain starts from the exobase altitude and no further ion-neutral or ion-ion collisions are allowed for in the current model. However, the study by *Barabash et al.* [2002] suggested that a significant fraction of oxygen ions may be converted to energetic neutral atoms (ENAs) through charge exchange collisions. Considering that ENAs are not affected by the electromagnetic fields, it is unclear how the collision process changes the probability of ions to escape. ENAs with a sufficient energy in an outward direction easily escape Mars, whereas those particles moving inward become more easily lost to the atmosphere. Nevertheless, the results presented in this work demonstrate the dominance of electromagnetic forces at controlling the escape rate of oxygen ions from the Mars upper atmosphere.

[31] It has been illustrated in this paper that whether atomic oxygen ions (O^+) are able to escape Mars depends on not only their kinetic energies, but also the electromagnetic

field distribution as well as particle locations. It is reasonable to expect that the distribution of molecular oxygen ions (O_2^+) above the exobase is also affected by the electromagnetic environment in the context of the Mars-solar wind interaction. A hemispheric asymmetry in the O_2^+ ion distribution is likely to exist. Considering that dissociative recombination of O_2^+ ions is the most important photochemical escape mechanism [*Lammer and Bauer*, 1991; *Fox*, 1993; *Zhang et al.*, 1993; *Krestyanikova and Shematovich*, 2006], it is interesting to investigate how the electromagnetic fields in the vicinity of Mars influence the photochemical escape rate and thus modify the photochemical state of the low-altitude atmosphere [*Nair et al.*, 1994].

[32] **Acknowledgments.** The work at the University of Colorado was supported by NASA grants NNX07AR04G and NNX08AP98G, and NSF grant AST-0908472. Resources supporting this work were provided by the NASA High-End Computing Program through the NASA Advanced Supercomputing Division at Ames Research Center.

[33] Wolfgang Baumjohann thanks Joseph Grebowsky and another reviewer for their assistance in evaluating this paper.

References

Acuña, M. H., et al. (1998), Magnetic field and plasma observations at Mars: Initial results of the Mars Global Surveyor mission, *Science*, *279*, 1676–1680.

Arkani-Hamed, J. (2001), A 50-degree spherical harmonic model of the magnetic field of Mars, *J. Geophys. Res.*, *106*(E10), 23,197–23,208.

Barabash, S., M. Holmström, A. Lukyanov, and E. Kallio (2002), Energetic neutral atoms at Mars 4. Imaging of planetary oxygen, *J. Geophys. Res.*, *107*(A10), 1280, doi:10.1029/2001JA000326.

Barabash, S., et al. (2007a), Martian atmospheric erosion rates, *Science*, *315*, 501–503.

Barabash, S., et al. (2007b), The loss of ions from Venus through the plasma wake, *Nature*, *450*, 650–653.

Brain, D. A., J. S. Halekas, R. Lillis, D. L. Mitchell, R. P. Lin, and D. H. Crider (2005), Variability of the altitude of the Martian sheath, *Geophys. Res. Lett.*, *32*, L18203, doi:10.1029/2005GL023126.

Brecht, S. H. (1997), Hybrid simulations of the magnetic topology of Mars, *J. Geophys. Res.*, *102*(A3), 4743–4750.

Carr, M. H., and H. Wänke (1992), Earth and Mars: Water inventories as clues to accretional histories, *Icarus*, *98*, 61–71.

Cravens, T. E., A. Hoppe, S. A. Ledvina, and S. McKenna-Lawlor (2002), Pickup ions near Mars associated with escaping oxygen atoms, *J. Geophys. Res.*, *107*(A8), 1170, doi:10.1029/2001JA000125.

Crider, D. H., et al. (2002), Observations of the latitude dependence of the location of the Martian magnetic pileup boundary, *Geophys. Res. Lett.*, *29*(8), 1170, doi:10.1029/2001GL013860.

Dubinin, E., M. Fraenz, J. Woch, F. Duru, D. Gurnett, R. Modolo, S. Barabash, and R. Lundin (2009a), Ionospheric storms on Mars: Impact of the corotating interaction region, *Geophys. Res. Lett.*, *36*, L01105, doi:10.1029/2008GL036559.

Dubinin, E., M. Fraenz, J. Woch, S. Barabash, and R. Lundin (2009b), Long-lived auroral structures and atmospheric losses through auroral flux tubes on Mars, *Geophys. Res. Lett.*, *36*, L08108, doi:10.1029/2009GL038209.

Ergun, R. E., L. Andersson, W. K. Peterson, D. Brain, G. T. Delory, D. L. Mitchell, R. P. Lin, and A. W. Yau (2006), Role of plasma waves in Mars' atmospheric loss, *Geophys. Res. Lett.*, *33*, L14103, doi:10.1029/2006GL025785.

Fang, X., M. W. Liemohn, A. F. Nagy, Y. Ma, D. L. De Zeeuw, J. U. Kozyra, and T. H. Zurbuchen (2008), Pickup oxygen ion velocity space and spatial distribution around Mars, *J. Geophys. Res.*, *113*, A02210, doi:10.1029/2007JA012736.

Fang, X., M. W. Liemohn, A. F. Nagy, J. G. Luhmann, and Y. Ma (2010), On the effect of the Martian crustal magnetic field on atmospheric erosion, *Icarus*, *206*, 130–138, doi:10.1016/j.icarus.2009.01.012.

Fedorov, A., et al. (2006), Structure of the Martian wake, *Icarus*, *182*, 329–336.

Fox, J. L. (1993), On the escape of oxygen and hydrogen from Mars, *Geophys. Res. Lett.*, *20*, 1847–1850.

Harnett, E. M., and R. M. Winglee (2006), Three-dimensional multifluid simulations of ionospheric loss at Mars from nominal solar wind conditions to magnetic cloud events, *J. Geophys. Res.*, *111*, A09213, doi:10.1029/2006JA011724.

Hartle, R. E., and J. M. Grebowsky (1995), Planetary loss from light ion escape on Venus, *Adv. Space Res.*, *15*, 117–122.

Johnson, R. E. (1994), Plasma-ion sputtering of an atmosphere, *Space Sci. Rev.*, *69*, 215–253.

Kallio, E., and P. Janhunen (2002), Ion escape from Mars in a quasi-neutral hybrid model, *J. Geophys. Res.*, *107*(A3), 1035, doi:10.1029/2001JA000090.

Kallio, E., and H. Koskinen (1999), A test particle simulation of the motion of oxygen ions and solar wind protons near Mars, *J. Geophys. Res.*, *104*(A1), 557–579.

Krestyanikova, M. A., and V. I. Shematovich (2006), Stochastic models of hot planetary and satellite coronas: A hot oxygen corona of Mars, *Sol. Syst. Res.*, *40*, 384–392.

Lammer, H., and S. J. Bauer (1991), Nonthermal atmospheric escape from Mars and Titan, *J. Geophys. Res.*, *96*, 1819–1825.

Leblanc, F., and R. E. Johnson (2001), Sputtering of the Martian atmosphere by solar wind pick-up ions, *Planet. Space Sci.*, *49*, 645–656.

Li, L., and Y. Zhang (2009), Model investigation of the influence of the crustal magnetic field on the oxygen ion distribution in the near Martian tail, *J. Geophys. Res.*, *114*, A06215, doi:10.1029/2008JA013850.

Lichtenegger, H., K. Schwingenschuh, E. Dubinin, and R. Lundin (1995), Particle simulation in the Martian magnetotail, *J. Geophys. Res.*, *100*(A11), 21,659–21,668.

Luhmann, J. G. (1990), A model of the ion wake of Mars, *Geophys. Res. Lett.*, *17*(6), 869–872.

Luhmann, J. G., and J. U. Kozyra (1991), Dayside pick-up oxygen ion precipitation at Venus and Mars: Spatial distributions, energy deposition, consequences, *J. Geophys. Res.*, *96*(A4) 5457–5467.

Lundin, R., et al. (1990), ASPERA/Phobos-2 measurements of the ion outflow from the Martian ionosphere, *Geophys. Res. Lett.*, *17*(6), 873–876.

Lundin, R., et al. (2004), Solar wind-induced atmospheric erosion at Mars: First results from ASPERA-3 on Mars Express, *Science*, *305*, 1933–1936.

Ma, Y., A. F. Nagy, I. V. Sokolov, and K. C. Hansen (2004), Three-dimensional, multispecies, high spatial resolution MHD studies of the solar wind interaction with Mars, *J. Geophys. Res.*, *109*, A07211, doi:10.1029/2003JA010367.

Mitchell, D. L., R. P. Lin, C. Mazelle, H. Reme, P. A. Cloutier, J. E. P. Connerney, M. H. Acuña, and N. F. Ness (2001), Probing Mars' crustal magnetic field and ionosphere with the MGS Electron Reflectometer, *J. Geophys. Res.*, *106*(E10), 23,419–23,427.

Modolo, R., G. M. Chanteur, E. Dubinin, and A. P. Matthews (2005), Influence of the solar EUV flux on the Martian plasma environment, *Ann. Geophys.*, *23*, 433–444.

Nagy, A. F., M. W. Liemohn, J. L. Fox, and J. Kim (2001) Hot carbon densities in the exosphere of Mars, *J. Geophys. Res.*, *106*(A10), 21,565–21,568.

Nair, H., M. Allen, A. D. Anbar, and Y. L. Yung (1994) A photochemical model of the Martian atmosphere, *Icarus*, *111*, 124–150.

Verigin, M. I., et al. (1991), Ions of planetary origin in the Martian magnetosphere (Phobos-2/Taus experiment), *Planet. Space Sci.*, *39*, 131–137.

Verigin, M., D. Vignes, D. Crider, J. Slavin, M. Acuña, G. Kotova, and A. Remizov (2004), Martian obstacle and bow shock: Origins of boundaries anisotropy, *Adv. Space Res.*, *33*, 2222–2227, doi:10.1016/S0273-1177(03)00522-2.

Zhang, M., J. G. Luhmann, S. W. Bougher, and A. F. Nagy (1993), The ancient oxygen exosphere of Mars: Implications for atmospheric evolution, *J. Geophys. Res.*, *98*(E6), 10,915–10,924.

X. Fang, Laboratory for Atmospheric and Space Physics, University of Colorado at Boulder, Boulder, CO 80309-0392, USA. (xiaohua.fang@lasp.colorado.edu)

M. W. Liemohn and A. F. Nagy, Space Physics Research Laboratory, University of Michigan, 2455 Hayward Street, Ann Arbor, MI 48109, USA.

J. G. Luhmann, Space Sciences Laboratory, University of California, Berkeley, CA 94720, USA.

Y. Ma, Institute of Geophysics and Planetary Physics, University of California, Los Angeles, CA 90095, USA.